INTERNATIONAL JOURNAL FOR NUMERICAL METHODS IN FLUIDS, VOL. 9, 1431–1451 (1989)

PROBABILISTIC APPROACH FOR TRANSPORT OF CONTAMINANTS THROUGH POROUS MEDIA*

M. C. ROCO, J. KHADILKAR AND J. ZHANG

Department of Mechanical Engineering, University of Kentucky, Lexington, KY 40506, U.S.A.

SUMMARY

The channels formed between individual particles in porous media have variable dimensions and orientations. The porosity, permeability and its anisotropy exhibit random spatial distributions. The probabilistic approach can effectively describe the transport of contaminants through porous media and is analysed in this paper. Numerical results are obtained by considering (I) random dispersion coefficients without and with spatial structure, (II) random time distribution of concentration at the inlet boundary, (III) random velocity distribution in the flow field without and (IV) with variable dispersion coefficient, (V) non-linearity of the governing equation and (VI) anisotropy of the dispersion coefficient. Two methods are used for probabilistic predictions: (1) Gaussian field approach in conjunction with Monte Carlo method and (2) random walk method. The input random parameters are assumed to have normal and log-normal distributions according to available experimental data. The probability distribution functions of the contaminant concentration at different locations within the flow domain are calculated and compared with the input distributions as a function of the mean and fluctuation Peclet numbers. The one-dimensional case is analysed in detail and the illustrative numerical predictions are compared with analytical and experimental results. The extension to a two-dimensional domain is discussed in the last part of this paper.

KEY WORDS Probabilistic diffusion–convection equation Gaussian field approach Random walk method Fluctuation Peclet number Porous media Two-phase system

1. PROBLEM DEFINITION AND OBJECTIVES

Motivation

The channels formed between individual particles in porous media have variable dimensions and orientations even for spherical particles of the same size. The mean field properties such as porosity, permeability, etc. of an assembly of particles within a control volume also exhibit a probabilistic character, which should be reflected in the computational algorithms. The probabilistic approach can effectively describe the flow mechanism and predict both mean and fluctuating quantities.

In a flowing mixture of solids and fluid the velocity, concentration and phase configurations are randomly distributed in space and time. In porous media the phase configuration and concentration are fixed in time, with spatial randomness. This makes porous media flow a good starting test case for more complex fluid–solid mixture flows, which are a longer-range objective of this study. Most of the previous work in the area of flow through porous media can be classified as

* Paper presented at the ASME Winter Annual Meeting, December 1987.

0271–2091/89/121431–21$10.50

Received 14 March 1988
Revised 22 December 1988

using the deterministic approach.[1-4] There are relatively fewer publications on probabilistic predictive methods for porous media flow, as well as for two-phase flows. Warren and Price[5] and Smith and Freeze[6] used Monte Carlo simulation techniques for saturated flow. Tang and Pinder[7] adopted perturbation theory for the numerical solution of the stochastic flow equation. Bakr *et al.*[8] proposed spectral analysis techniques for spatial stochastic processes characterized by covariance functions.

The work presented here deals with the transport of contaminants through porous media by using a probabilistic approach. The main objective is to show some qualitative trends in probabilistic field analysis of the macroscopic equations. Accordingly, simple flow situations are preferred for analysis as asymptotic case studies for possible applications. The dependence of the dispersion coefficient on the particle size constituting the porous medium has been obtained from the experiments of Rummer *et al.*[9-11] for the illustrative computational tests. The experimental relation between the concentration and mean flow Peclet number discussed by Lavenspiel and Smith[12] was used for comparison in this work.

Generally, the probabilistic approach has two steps:

(a) Micromechanical analysis of the flow around individual particles within a local control volume, from which the probability distribution functions for the field parameters are obtained (for instance, for the dispersion coefficient as a function of particle size and spatial arrangement);
(b) Field analysis, in which the field parameters are used as input data to calculate the probability distribution functions of the field solutions (such as concentration in a flow domain). The field parameters may be functions of porous medium and flow conditions (velocity, local velocity gradient, concentration gradient, etc.). The objective of this paper is the field analysis. The input probability distribution functions of the field parameters were assumed based on experimental correlations in our illustrative computations.

Direct simulation is the most accurate approach to obtain the probability distribution function of the field solution. This approach is used in the present work. However, for complex problems in two- and three-dimensional domains it is justifiable to adopt more time-efficient numerical techniques, which would be a compromise between the full probabilistic description of the flow mechanism and computer time efficiency. The finite element, finite volume and other deterministic numerical methods can be reformulated within a stochastic framework by adding the probabilistic dimension into the analysis.[13-15]

The problem considered

We intend to determine the distribution of the probability density function of concentration in porous media within a given flow field by using the probabilistic approach via direct numerical simulation. The random input data are one or a combination of the field parameters attached to the porous medium, boundary conditions or initial conditions. The effect of the spatial dependence between neighbouring values of the field parameters is estimated. The flow without spatial dependence is considered as an asymptotic case. Qualitative effects of the input random parameters on the concentration distribution are investigated. Two probabilistic methods are used:

(1) Gaussian field approach in conjunction with Monte Carlo method
(2) random walk method.

The solutions of these two methods are compared with the deterministic numerical solutions and available experimental results.

2. PROBABILISTIC MODEL

Basic equations

Transport of a contaminant. The macroscopic instantaneous governing equation for the diffusion–convection process written in non-dimensionalized form is

$$\frac{\partial C^*}{\partial t^*} + u_i^* \frac{\partial C^*}{\partial x_i^*} - \frac{\partial}{\partial x_i^*}\left(\frac{1}{Pe_{\text{mean},i}} \frac{\partial C^*}{\partial x_i^*}\right) + S_c^* = 0, \tag{1}$$

where $C^* = (C - C_b)/(C_0 - C_b)$; $t^* = t\,U/L$; $x^* = x/L$; $u_i^* = u_i/U$; S_c^* is the source term (non-dimensionalized); $Pe_{\text{mean},i} = U\,L/D_i$ (mean flow Peclet number in the ith direction); D_i is the dispersion coefficient for C in the $i = x$-, y- or z-direction respectively; U is the reference mean velocity; L is the length of the domain; C is the concentration as a function of the position vector $\mathbf{x}$ and time, $C(\mathbf{x}, t)$; C_b is the concentration at boundary $x = 0$; C_0 is the initial concentration; t is time; x_i is the cartesian co-ordinate (x, y or z); and u_i is the seepage velocity in the $i = x$-, y- or z-direction respectively.

The boundary conditions are

$$A \frac{1}{Pe_i} \frac{\partial C^*}{\partial x_i^*} + B u_i^* n_i C^* = 1, \tag{2}$$

where A, B and n_i define the physical conditions (n_i is the projection of the unit normal vector to the boundary on the ith co-ordinate).

In the illustrative one-dimensional problem the concentration C is imposed at $x^* = 0$ and the gradient $\partial C^*/\partial x^*$ at $x^* = x^*_{\max}$. This equation is non-linear when D_i or u_i^* is a function of C^*. Anisotropy within the flow field is caused by the anisotropy of particle arrangement, which is reflected mainly on the anisotropy of the dispersion coefficient. The following parameters may be characterized by either probability distribution functions or constants: u_i^*, D_i, S_c^*, A, B, n_i.

Besides the mean flow Peclet number (Pe_{mean}) which is used in the deterministic analysis, the fluctuation or standard deviation Peclet number (Pe_{std}) is defined in this paper to characterize the fluctuating transport process in space and time. For a steady mean flow, Pe_{std} is defined as

$$Pe_{\text{std}} = \left[\sum_{j=1}^{N} (Pe_j - Pe_{\text{mean}})^2/N\right]^{0.5}, \tag{3}$$

where $Pe_j = u_j\,\Delta l/D_j = (u_{\text{mean}} + u_j')\Delta l/(D_{\text{mean}} + D_j')$ is the local instantaneous Peclet number (sample j); $Pe_{\text{mean}} = U_{\text{mean}}\,\Delta l/D_{\text{mean}}$; N is the number of samples (number of spatial intervals or time intervals, respectively); and Δl is the characteristic length of the fluctuating transport process. In a numerical method Δl may be the same as the mesh size.

By assuming D_j' very small compared with D_{mean}, which also implies $D_j'\,u_j' \ll D_{\text{mean}}\,u_j'$, one obtains

$$Pe_{\text{std}} = (u_{\text{std}} - u_{\text{mean}}\,(D_{\text{std}}/D_{\text{mean}}))\,\Delta l/D_{\text{mean}}. \tag{4}$$

The standard deviation Peclet number (4) can be defined over a domain in space ($Pe_{\text{std},s}$) or time ($Pe_{\text{std},t}$), or their combination. The mean flow and variance (or standard deviation) Reynolds numbers, Re_{mean} and Re_{std}, are defined in a similar way for the momentum equations.

Typical situations

Six typical situations are investigated numerically for equation (1) as listed in Table I: (1) random particle diameter distribution (D_i is also randomly distributed in space); (II) random boundary concentration (C at the boundary is randomly distributed in time); (III) random velocity (u_i^* is normally and log-normally distributed in space); (IV) random dispersion coefficient and velocity (D_i and u_i^* are both normally and log-normally distributed in space); (V) non-linearity of the governing equation (D_i and u_i^* are functions of C^*); (VI) anisotropy of the dispersion coefficient D_i or/and velocity u_i^* in a two-dimensional domain. The computational objective is to determine the probability distribution function of concentration (C^*) at different locations in the domain ($\mathbf{x}$) and various time intervals (t^*).

(*I*) *Random dispersion coefficient.* The particles constituting the porous media are assumed to be spheres. The distribution on the particle size is considered to be normal, with a mean d_{mean} and a standard deviation d_{std}. The relation among the dispersion coefficient D_i, sphere diameter d and seepage velocity u_i (given by Darcy's law) is taken for illustration from the experiments of

Table I. Test cases (with constant parameters $D_{x,\text{mean}} = 0{\cdot}06\,\text{cm}^2\,\text{s}^{-1}$, $C_{\text{b,mean}} = 0{\cdot}5$ vol. %, $u^*_{x,\text{mean}} = 1{\cdot}0$, $t^* = 0{\cdot}0618$)

Test case	Description	Input distribution	Computed concentration distribution
I	Varying D_x $C_b = C_{b,\text{mean}}$ $u_x = u_{x,\text{mean}}$	D_x normal in x	C normal
II	$D_x = D_{x,\text{mean}}$ Varying C_b $u_x = u_{x,\text{mean}}$	C_b normal in t	C normal
III	$D_x = D_{x,\text{mean}}$	a. u_x normal in x	C normal
	$C_b = C_{b,\text{mean}}$ Varying u_x	b. u_x log-normal in x	C log-normal
IV	Varying D_x $C_b = C_{b,\text{mean}}$	a. D_x normal in x u_x normal in x	C normal
		b. D_x normal in x u_x log-normal in x	C log-normal
V	Non-linear governing equation (D_x function of C)	D_x normal in x	C normal
VI	Two-dimensional anisotropic diffusion coefficient ($D_y = D_x/a$)	D_x normal in x	C normal

Rummer[9-11] (CGS units):

$$D_i = 1{\cdot}84\, u_i^{1{\cdot}2}\, u^{1{\cdot}2}. \tag{5}$$

Figure 1 shows two probability distribution functions f_D of the one-dimensional dispersion coefficient D_x, where $u_x = 0{\cdot}309\ \mathrm{cm\,s^{-1}}$, $d_{\mathrm{mean}} = 0{\cdot}2\ \mathrm{cm}$ and $D_{\mathrm{mean}} = 0{\cdot}06\ \mathrm{cm^2\,s^{-1}}$, which would correspond to the mean flow $Pe_{\mathrm{mean}} = 0{\cdot}515$. Two standard deviations of the dispersion coefficient are considered: $D_{\mathrm{std}} = 0{\cdot}001$ and $0{\cdot}005\ \mathrm{cm^2\,s^{-1}}$. These correspond to $Pe_{\mathrm{std}} = 0{\cdot}0086$ and $0{\cdot}043$, respectively.

Usually D_i is averaged over a small control volume. In numerical simulations D_i is averaged over the finite computational domain. Its non-uniformity as well as the anisotropy and spatial dependence between neighbouring values are diminished with an increase of the averaging volume,[16] even if the integral length scale λ (as defined in Reference 8) remains constant. In practical applictions it is important to relate the experimental technique for measuring D_i to the averaging volume used in analysis.

The spatial correlation for a quantity f is introduced in the one-dimensional calculation by using the autoregressive parameter α which takes values between 0 and 1:

$$f_i = \alpha(f_{i-1} + f_{i+1}) + g_i, \tag{6}$$

where f_{i-1} and f_{i+1} are two neighbouring values and g_i is a normal random variable uncorrelated with other g_j's.

(*II*) *Random boundary conditions.* In this case the random parameter is the time distribution of the point concentration C_b at the inlet boundary. The dispersion coefficient and velocity are constant within the flow domain. In the initial test cases we assume a normal distribution of C_b ($C_{b,\mathrm{mean}} = 0{\cdot}50$ vol.% with two values of the standard deviation, $C_{b,\mathrm{std}} = 0{\cdot}02$ and $0{\cdot}10$ vol.%).

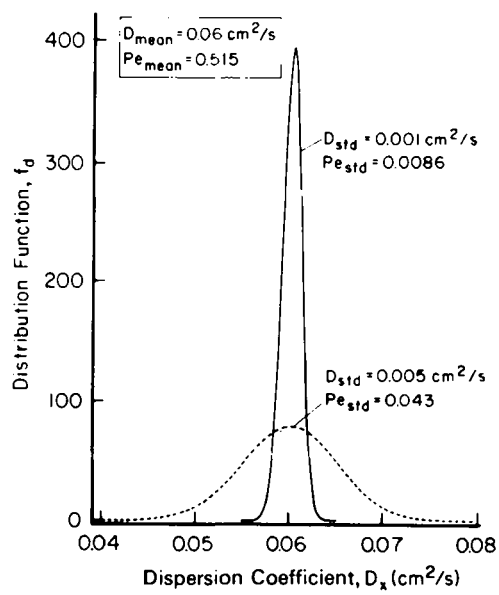

Figure 1. Input probability distribution function of the dispersion coefficient in space, f_D

(*III*) *Random velocity.* The dispersion coefficient and concentration at the inlet boundary are assumed constant within the flow domain, and the random parameter is the spatial distribution of the velocity u_i^*, which is a function of d^2.[9] The velocity u is given by Darcy's law:

$$u = \frac{k}{\theta}\frac{\gamma}{\mu}\frac{\mathrm{d}h}{\mathrm{d}x} = 7{\cdot}725\,d^2, \tag{7}$$

where k is the instrinsic permeability (function of d^2), θ is the porosity (function of shape and size distribution of particles), γ is the liquid specific weight and μ is the piezometric head.

In the initial test cases we assume a normal distribution of the velocity in the flow domain (case IIIa). Figure 2 shows the two probability distribution functions f_{u*} of the fluctuating velocity for $u^*_{\mathrm{mean}} = 1{\cdot}0$ and two values of the standard deviation, $u^*_{\mathrm{std}} = 0{\cdot}06$ and $0{\cdot}12$. Additional case studies with log-normal distributions of the velocity are also analysed for the same mean and standard deviations (case IIIb).

(*IV*) *Random dispersion coefficient and velocity.* This case is a combination of cases I and III. Both random parameters D_i and u_i^* are assumed to be normally distributed in space, with the probability distribution functions f_d and f_{u*}, respectively. An additional test case with D_i normally distributed and u_i^* log-normally distributed is also analysed.

(*V*) *Non-linearity of the governing equation* (*the dispersion coefficient and/or velocity are functions of concentration*). The non-linearity of the dispersion process through porous media occurs when the dispersion coefficient and/or velocity are a function of concentration. In the illustrative test cases the relation between the dispersion coefficient D_i and concentration C is estimated from the fluidization experiments of Richardson and Zaki:[17]

$$D_i = D_i^0\,(1 - C/C_{\mathrm{M}})^n, \tag{8}$$

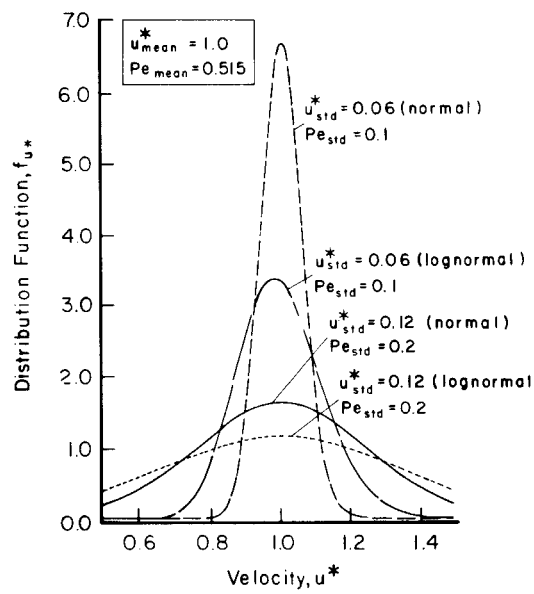

Figure 2. Input probability distribution function of the velocity in space, f_{u*}

where D_i is the random dispersion coefficient, dependent on concentration C, in the $i = \bar{x}$-, y- or z-direction respectively; D_i^0 is the random dispersion coefficient at $C = 0$; C and C_M are the concentration and maximum packing concentration respectively; and n is an experimental exponent.

A similar relationship to (8) can be considered between the velocity u_i and concentration C. The mean and the standard deviation of D_i and u_i required in the analysis are taken from cases I and III respectively. The inlet boundary concentration is assumed constant. In the illustrative cases the exponent n is taken to be equal to unity.

(*VI*) *Anisotropy of the dispersion coefficient and/or velocity.* The anisotropy and non-homogeneity of the particle arrangement cause the anisotropy of the dispersion coefficient as well as of the velocity. The effect can be represented in the random walk approach but cannot be represented in the Gaussian field approach. The diffusion coefficient and the velocity in the main flow direction are generally greater than the diffusion coefficient and the velocity in other directions. In the initial test cases both the random parameters are assumed to be normally distributed and their values in the main flow direction are twice the values in other directions. The mean value and the standard deviation of these two parameters are taken from cases I and III (D_i from case I and u_i^* from case III). The inlet boundary concentration is assumed constant.

3. GAUSSIAN FIELD APPROACH IN CONJUNCTION WITH MONTE CARLO METHOD

Proposed computational scheme

The Monte Carlo method proceeds by constructing a hypothetical model of population Ω, with its probability space (Ω, F, P). F is the Borel field consisting of certain subsets of Ω, and P is the set of probabilities assigned to each element of F. In the case of random particle distribution, Ω will represent all positive real numbers and F will represent its subsets consisting of a particular set of particle diameters. An unbiased primary estimator of the random parameter, $Z(\xi)$ with $\xi \in \Omega$, is sampled repeatedly and independently N times to yield a convergent secondary estimator S_N. The primary estimator $Z(\xi_i)$ is itself a random variable defined on (Ω, F, P). Its expectation is equal to the solution S_N and has finite standard deviation:[18]

$$S_N = \frac{1}{N} \sum_{i=0}^{N} Z(\xi_i). \tag{9}$$

In the case of the Gaussian field approach the chi-square goodness-of-fit test is used to fit a distribution to the output parameter. In this test we make a hypothesis that if one of the input parameters is normally or log-normally distributed (i.e. the diffusion coefficient, initial or boundary condition) with the remaining input parameters constant, then the solution process, i.e. concentration, may be represented by normal or log-normal distributions, respectively. The procedure to check whether the hypothesis is true or false is explained in detail for the one-dimensional case. The computational steps are:

(a) The analytical solution to the differential equation (1) with $S_c^* = 0$ for constant property values in the one-dimensional case is

$$C^* = 1 - 0{\cdot}5 \operatorname{erfc}\left(\frac{x^* - u_x^* t}{2(t^*/Pe)^{0{\cdot}5}}\right) \tag{10}$$

with the following initial and boundary conditions:

$$C^*(x, 0) = 1, \qquad x^* \geqslant 0,$$
$$C^*(0, t^*) = 0, \qquad t^* \geqslant 0,$$
$$C^*(\infty, t) = 1, \qquad t^* \geqslant 0,$$

where erfc ( ) is the complementary error function and t^* is time. Formula (10) is successively applied starting from $x = 0$ in each finite domain Δx with the corresponding random values of u_x^* and Pe.

(b) N different values of the system variable, i.e. concentration, are calculated at each location by using N random values of the input random parameter with the normal distribution.

(c) The hypothesis is checked using a chi-square goodness-of-fit test. If the test parameter, namely chi-square, is found to be above a certain critical limit, then the hypothesis is rejected, else it is assumed to be true. The chi-square goodness-of-fit test parameter χ^2 varies as a function of the input parameters and the number of iterations. In our tests, after 50 iterations it takes values between 5 and 11, after 200 iterations between 4 and 7, and after 500 iterations all values are less than 5.

Typical applications

Case I. Random dispersion coefficient D_i. In the case of random particle size distribution we generate N random particle diameters with a given distribution. In the illustrative test cases the particle diameter is assumed to have a normal random distribution with a mean diameter of 0·2 cm.[9] With these N different random values of d, N different values of the dispersion coefficients are calculated using the experimental relation (5).

The differential equation (1) governing the process is solved with these random values of the dispersion coefficients. The solution is given by equation (9). The second, third and fourth moments of the system variable are also calculated. The mean value or the expectation of the system variable (concentration) is then compared with the deterministic numerical solution and available experimental results. The calculated probability distribution function f_{C*} for varying D_x and $\alpha = 0$ is plotted in Figure 3. The results are given at two locations, $x^* = 0{\cdot}04$ and 0·1, at time $t^* = 0{\cdot}0618$. Figure 4 shows the mean and standard deviation of concentration (C^*_{mean} and C^*_{std}) for varying dispersion coefficient. By increasing the autoregressive parameter α, the contaminant propagates slightly faster with a significant increase of C^*_{std}.

Case II. Random boundary condition C_b. The same procedure is followed for random initial or boundary condition as in the case of random particle diameter. N different random values of the initial concentration are generated according to the given distribution, and the equation governing the process (1) is solved N times using these random values. Figure 5 shows the standard deviation of concentration along x^* at $t^* = 0{\cdot}0618$. The mean concentration distribution is similar to Figure 4(a).

Case III. Random velocity u^*. N different random values of the velocity are generated with the given probability distribution (normal and log-normal). The calculated probability distribution function f_{C*} for fluctuating velocity u^* is plotted in Figure 6. The results are given at two locations, $x^* = 0{\cdot}04$ and 0·1, at $t^* = 0{\cdot}0618$. Figure 7 shows the standard deviation of concentration. The curve $C^*_{\text{mean}}(x^*)$ is similar to cases I (Figure 4(a)) and II because $Pe_{\text{mean}} = 0{\cdot}515$ is the same.

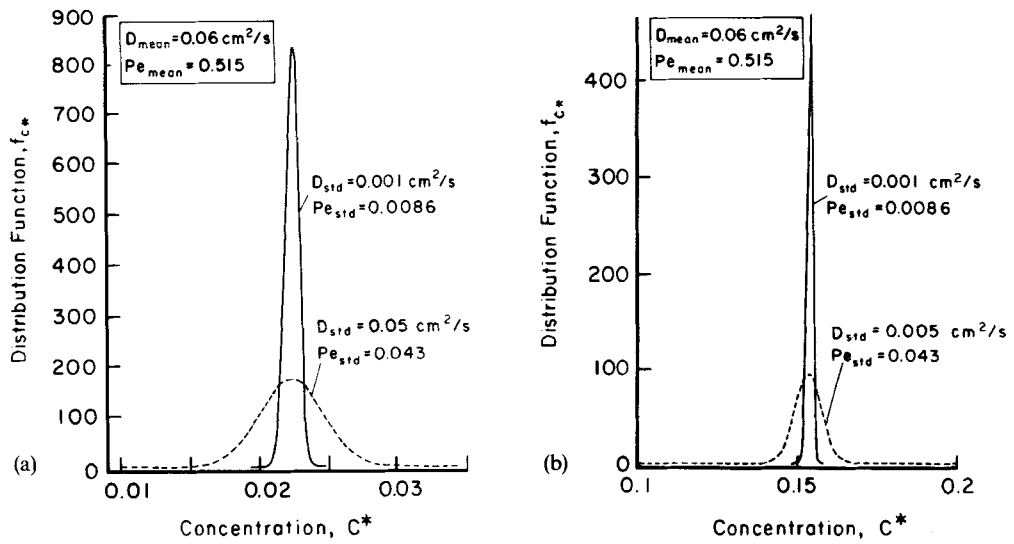

Figure 3. Calculated distribution function of concentration, f_{C*}, at $t^* = 0{\cdot}0618$ for the distribution of D_x from Figure 1: (a) $x^* = 0{\cdot}04$; (b) $x^* = 0{\cdot}1$

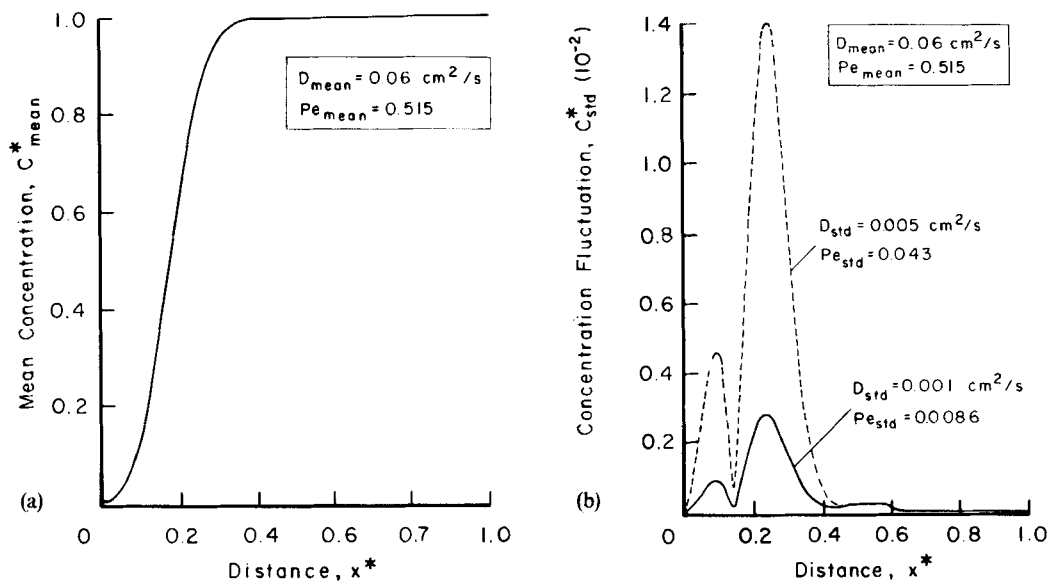

Figure 4. Calculated distribution of concentration along x^* at $t^* = 0{\cdot}0618$ for the distribution of D_x from Figure 1: (a) C^*_{mean}; (b) C^*_{std}

Case IV. Random dispersion coefficient D_i, random velocity u_i^*. Both parameters are generated randomly N times with the given probability distributions from cases I and III. Then the governing differential equation (1) is solved N times and the expectation of the solution represents the concentration. Figure 8 shows the standard deviation of concentration for random D_i and u_i^*. Pe_{mean} is equal to 0·515 and then the mean concentration distribution is similar to Figure 4(a).

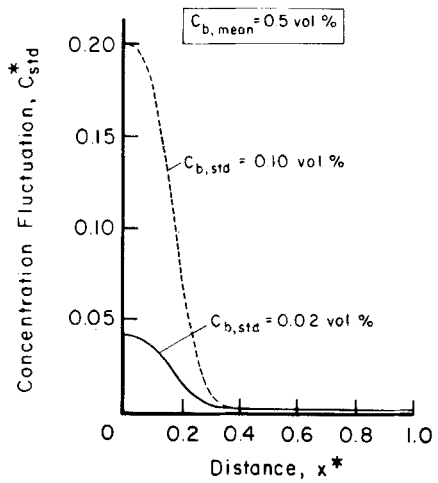

Figure 5. Calculated C^*_{std} along x^* at $t^* = 0{\cdot}0618$ for fluctuating concentration at $x^* = 0$

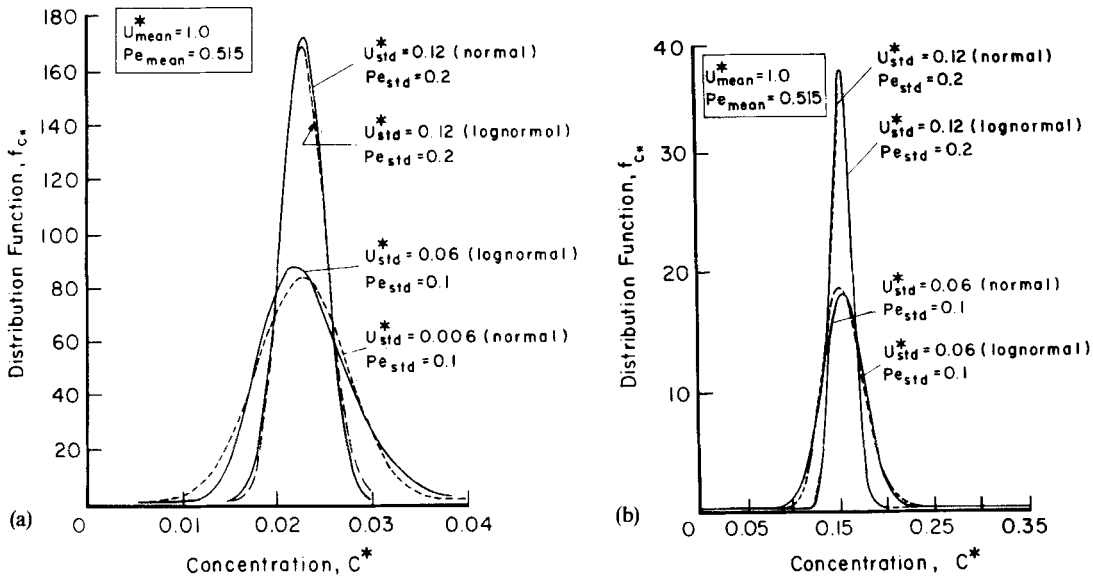

Figure 6. Calculated distribution function of concentration, f_{C^*}, at $t^* = 0{\cdot}0618$ for the velocity distribution from Figure 2: (a) $x^* = 0{\cdot}04$; (b) $x^* = 0{\cdot}1$

Case V. Non-linearity of the governing equation (dispersion coefficient and/or velocity are functions of concentration). The dispersion coefficient D_i and velocity u_i depend on the contaminant concentration C (equation (8)). The non-linear equation is solved via the direct iteration approach.[19] The random parameter is generated N times according to the input probability distribution. Then the governing differential equation (1) is solved N times. The procedure is repeated until the solution converges. Figure 9 shows the calculated mean and standard deviation of concentration for non-linear D_i. Both curves are affected by the ratio C_b/C_M.

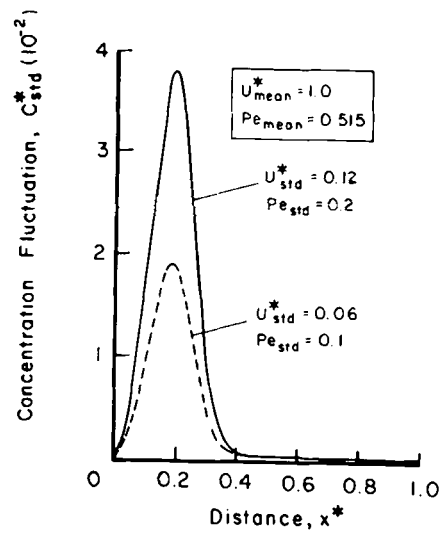

Figure 7. Calculated C^*_{std} along x^* at $t^* = 0{\cdot}0618$ for the velocity distribution from Figure 3

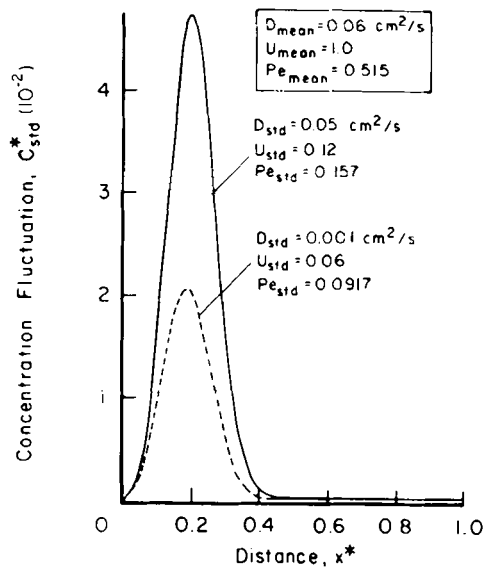

Figure 8. Calculated C^*_{std} along x^* at $t^* = 0{\cdot}0618$ for the dispersion coefficient distribution from Figure 1 and the velocity distribution from Figure 3

In the initial test cases for the Gaussian field approach (cases I and II in Table I) the distribution of the input parameter is normal. In case III the random parameter (velocity) distribution is normal as well as log-normal. It was found with the chi-square goodness-of-fit test that the output variable (concentration) has a normal distribution with 80% confidence level when the input parameters D_i, C_b and u_i are normally distributed. Pe_{mean} and Pe_{std} (defined in equation (3)) can be correlated to the mean values and standard deviations of concentration, respectively. Figures 10

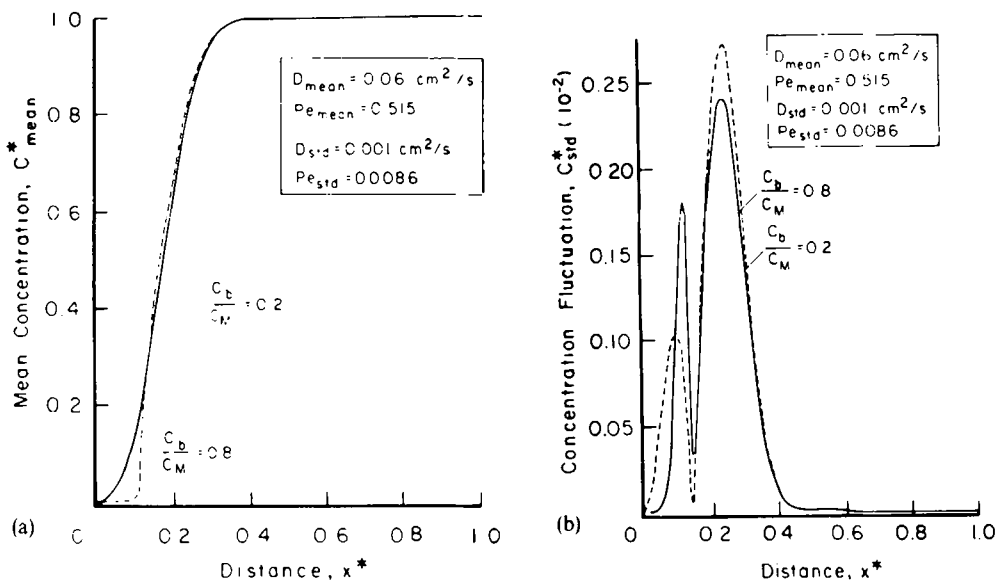

Figure 9. Calculated distribution of concentration along x^* at $t^* = 0.0618$ for non-linear governing equation: (a) C^*_{mean}; (b) C^*_{std}

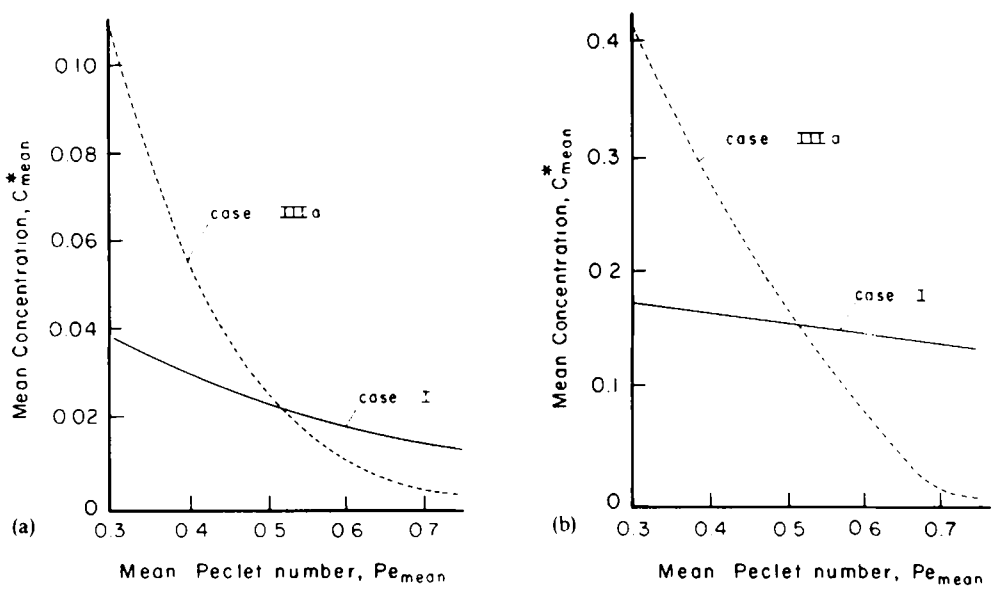

Figure 10. C^*_{mean} versus Pe_{mean} at $t^* = 0.0618$ for cases I and IIIa: (a) $x^* = 0.04$; (b) $x^* = 0.1$

and 11 illustrate the effect of Pe_{mean} on C^*_{mean} and C^*_{std} respectively for cases I and IIIa at two locations, $x^* = 0.04$ and 0.1, at time $t^* = 0.0618$. While Pe_{mean} affects the gradient of C^*_{mean}, the concentration fluctuations C^*_{std} appear to increase in direct proportion to Pe_{std} (Figures 12 and 13). C^*_{std} also increases with the spatial dependence expressed by the autoregression parameter α (Figure 13). The variation is quasilinear for normal distribution functions (Figure 13(a)) and flattens for log-normal distributions (Figure 13(b)).

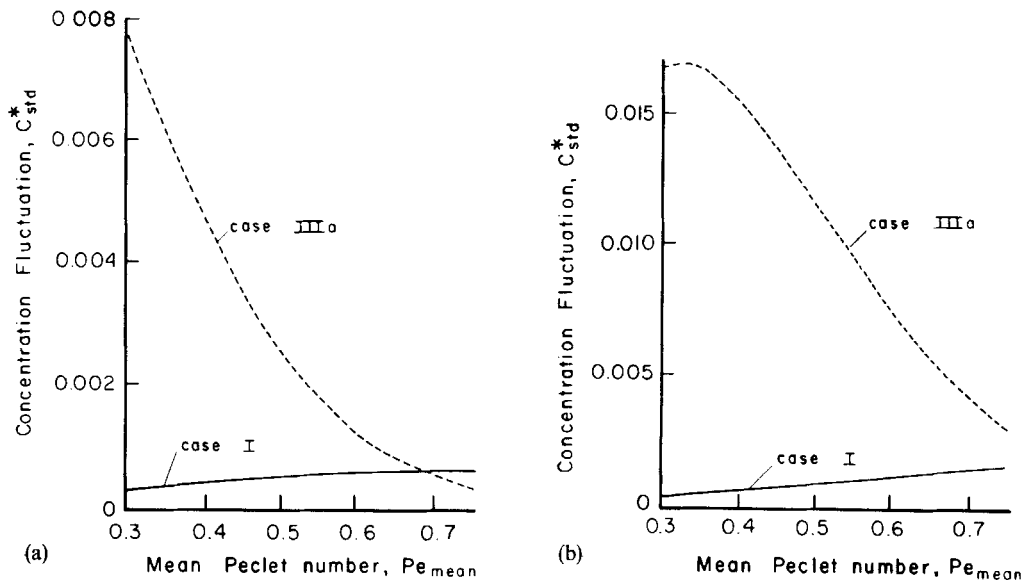

Figure 11. C^*_{std} versus Pe_{mean} at $t^* = 0{\cdot}0618$ for cases I and IIIa: (a) $x^* = 0{\cdot}04$; (b) $x^* = 0{\cdot}1$

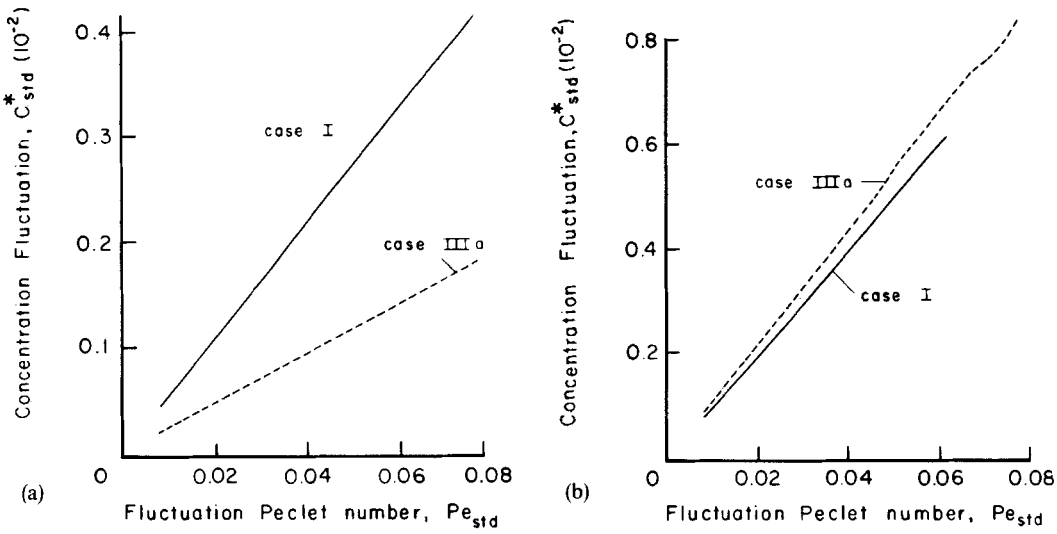

Figure 12. C^*_{std} versus Pe_{std} at $t^* = 0{\cdot}0618$ for cases I and IIIa: (a) $x^* = 0{\cdot}04$; (b) $x^* = 0{\cdot}1$

4. RANDOM WALK APPROACH

Proposed computational scheme

In the random walk approach the solution process is assumed to have a random path in the given domain.[20] In particular, if the solution process is at a point $\mathbf{x}_i$, in the next time step it can go to any of the directions j, where $j = 1, j_{max}$, with a probability of a_j, where $\Sigma_{j=1}^{j_{max}} a_j = 1$. If the

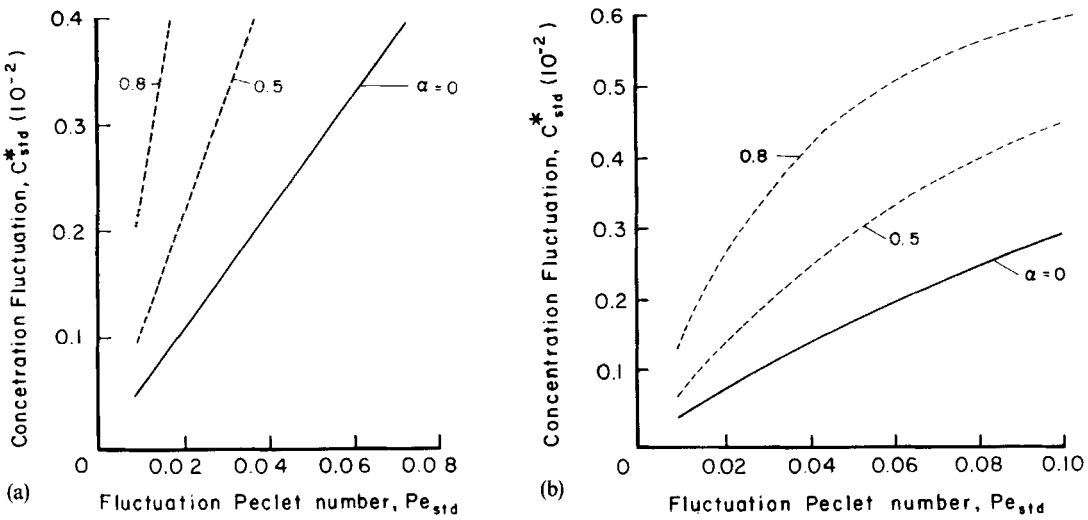

Figure 13. C^*_{std} versus Pe_{std} at $t^* = 0{\cdot}0618$ and $x^* = 0{\cdot}04$ for various autoregressive parameters α: (a) case I; (b) case IIIb

solution process is at the origin, then the probability of going in the negative co-ordinate direction is assumed to be zero. Each step in space is a backward step in time. The random walk generally terminates after s_{max} steps. When the solution process hits any of the boundaries in s_{max} or less steps, the process or the walk is terminated and an appropriate value is registered as $Z(\xi_m)$, m being the mth random walk. After the termination of the walk the process is again started from the point $\mathbf{x}_i$. M such different and independent random walks are performed starting at $\mathbf{x}_i$. ξ_m represents the mth random walk and $Z(\xi_m)$ represents the appropriate number tallied on termination of the mth walk. Then $Z(\xi_m)$ is the primary estimator of the solution at $\mathbf{x}_i$ and S_M given by an equation similar to (9) is the final approximation to the solution.[18] The α_j are the coefficients of the finite difference representation of the differential equation governing the process. The one-dimensional case of equation (1) with $S^*_c = 0$ and $\partial Pe_{mean,x}/\partial x^* = 0$ is

$$\frac{\partial C^*}{\partial t^*} + u^*_x \frac{\partial C^*}{\partial x^*} - \frac{1}{Pe_{mean,x}} \frac{\partial^2 C^*}{\partial x^{*2}} = 0. \tag{11}$$

The finite difference form of equation (11) about a starting point i is

$$C^*(X^*_i, t^*) = \sum_{j=i}^{2} \alpha_j C^*(X^*_j, t^*), \tag{12}$$

where X^*_i is the co-ordinate of the starting point i, X^*_j are the co-ordinates of neighbouring points j, where $j = 1, j_{max}$,

$$\alpha_1 = \frac{(1/Pe_x) - h^* u^*_x}{2(1/Pe_x) - h^* u^*_x}, \tag{13a}$$

$$\alpha_2 = \frac{1/Pe_x}{2(1/Pe_x) - h^* u^*_x}, \tag{13b}$$

$Pe_x = U L/D_x$, L is the length of the domain, u^*_x is the velocity in the x-direction, D_x is the dispersion coefficient in the x-direction and h^* is the non-dimensional step increment.

The step size chosen for the random walk method has an upper bound. It can be determined from the fact that $1 \geqslant \alpha_j \geqslant 0$ for all j. This condition gives us

$$0 \leqslant h^* \leqslant 1/(Pe_x u_x^*). \tag{14}$$

In the computational tests for the random walk method presented in this paper, we have $h^* = 0{\cdot}01$, with the condition $h^* \leqslant 0{\cdot}019$ (unless otherwise specified), and $M = 1000$. The results for C^*_{mean} and C^*_{std} in the one-dimensional case studies are similar to the Monte Carlo method.

Typical applications

The series of input data used for the Gaussian field approach (cases I–V) are also considered for the random walk method. The solutions were obtained for different h (step length) and M (number of walks).

The moment of order n of a random variable w with its probability density function f_w is

$$\overline{w^n} = \int_{-\infty}^{+\infty} w^n f_w \, dw. \tag{15}$$

The third moment (skewness) represents the asymmetry of the distribution and the fourth moment (kurtosis) represents its flatness or steepness. Tables II ($\alpha = 0$) and III ($\alpha \geqslant 0$) compares these four moments of the input and output parameters for the test cases discussed above. It is clear from Table III that the second moments increase with α, i.e. the fluctuation becomes stronger with the spatial correlation. The skewness increases with α in case I but decreases in case IIIb. The kurtosis decreases in both cases while α increases.

When the governing differential equation is non-linear (D_i and/or u_i^* are functions of concentration), the calculated mean concentration curve is flatter at the start of the domain for $C_b/C_M = 0{\cdot}8$ compared to the case where $C_b/C_M = 0{\cdot}2$. The second moment (standard deviation)

Table II. Moments of the input and computed parameters at distance $x^* = 0{\cdot}1$ and time $t^* = 0{\cdot}0618$ for $\alpha = 0$

Test case		w	Random input parameter (w)				Output parameter (C^*)			
			$\overline{w^{*1}}$	$\overline{w^{*2}}$	$\overline{w^{*3}}$	$\overline{w^{*4}}$	$\overline{C^{*1}}$	$\overline{C^{*2}}$	$\overline{C^{*3}}$	$\overline{C^{*4}}$
I	Random dispersion coefficient	D_x	0·06	0·001	−0·05	−0·5	0·15	0·0008	−0·1	−0·5
			0·06	0·005	−0·05	−0·5	0·15	0·004	−0·4	−0·3
II	Random boundary condition	C_b	0·5	0·02	−0·05	−0·5	0·15	0·03	0·3	−0·3
			0·5	0·10	−0·05	−0·5	0·15	0·07	0·03	−0·3
			a. Normal distribution							
III	Random transport velocity	u_x^*	1·0	0·06	−0·05	−0·5	0·15	0·03	0·3	−0·4
			1.0	0·12	−0·05	−0·5	0·16	0·05	0·5	−0·3
			b. Log-normal distribution							
		u_x^*	1.0	0·06	−0·04	−0·5	0·14	0·015	−1·90	3·90
			1.0	0·12	−0·01	−0·5	0·13	0·026	−1·61	2·60

Table III. Moments of the input and computed parameters at distance $x^* = 0{\cdot}1$ and $t^* = 0{\cdot}0618$ for $\alpha \geqslant 0$

	Test case	α	Random input parameter (w)					Output parameter (C^*)			
			w	$\overline{w^{*1}}$	$\overline{w^{*2}}$	$\overline{w^{*3}}$	$\overline{w^{*4}}$	$\overline{C^{*1}}$	$\overline{C^{*2}}$	$\overline{C^{*3}}$	$\overline{C^{*4}}$
I	Random dispersion coefficient	0	D_x	0·06	0·001	−0·05	−0·5	0·15	0·0008	−0·12	−0·48
		0·5						0·15	0·0017	−0·19	−0·46
		0·8						0·15	0·0042	−0·39	−0·32
IIIb	Random transport velocity (log-normal distribution	0	u_x^*	1.0	0·06	−0·04	−0·5	0·14	0·0147	−1·90	3·90
		0·5						0·13	0·0256	−1·61	2·61
		0·8						0·10	0·0396	−0·75	−0·42

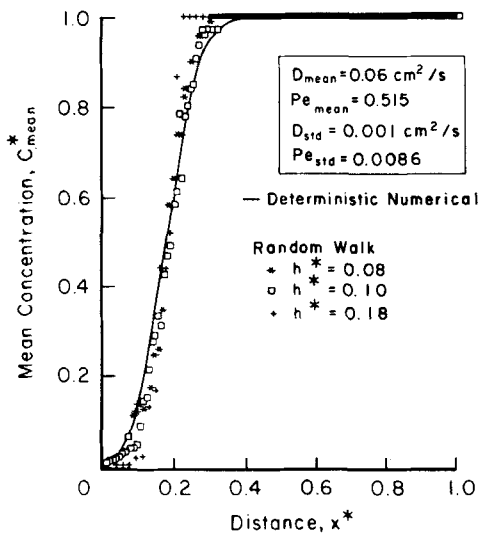

Figure 14. Calculated distribution of concentration along x^* at $t^* = 0{\cdot}0618$ (random walk approach with $M = 1000$)

and third moment (skewness) are also larger in the first case compared to the second case. The fourth moment (kurtosis) increases as the standard deviation of the input random parameter increases in the first case ($C_b/C_M = 0{\cdot}8$) but has less effect in the second case when $C_b/C_M = 0{\cdot}2$.

The accuracy of the solution with the random walk method depends on two main parameters, namely h^* (step length) and M (number of walks). Figure 14 shows that as h^* decreases, the solution approaches the expected solution. The optimum value of M is found to be 1000 walks.

Extension to two-dimensional case

The mean flow velocity is assumed to be in the x direction, while in the y direction there are only the fluctuating components. The dispersion coefficient in the y direction is $D_y = D_x/a$, where D_x is determined from equation (5) and a is the anisotropy coefficient.

Case VI. Anisotropy of the dispersion coefficient. In two-dimensional domains the anisotropy of the disperson coefficient plays an important role because of the non-homogeneous nature of the particle arrangement. In the initial test cases the coefficient of anisotropy a is taken to be 2·0. The initial and boundary conditions for this test case are given in Figure 15. The results for different values of the anisotropy coefficient a at $x^* = 0{\cdot}5$ are presented in Figure 16.

In this section only specific changes in the probabilistic algorithm for the two-dimensional case are mentioned. The finite difference form of the two-dimensional dispersion–convection equation (1) with $S_c^* = 0$ and $\partial D_i/\partial x_i^* = 0$ about a node i in the two-dimensional mesh is

$$C^*(X_i^*, t^*) = \sum_{j=1}^{4} \alpha_j C^*(X_j^*, t^*), \tag{16a}$$

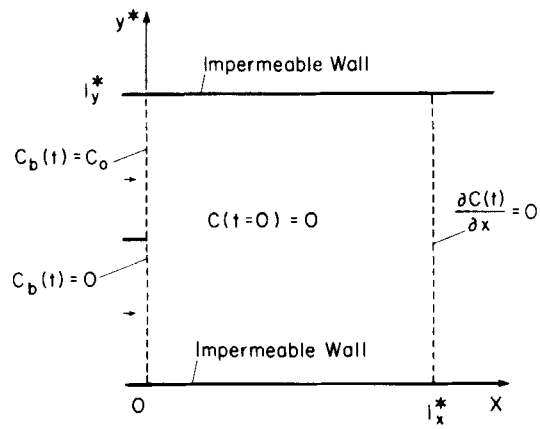

Figure 15. Initial and boundary conditions for case VI

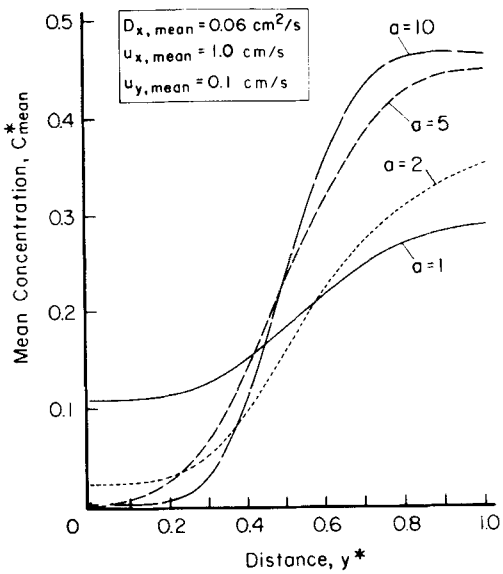

Figure 16. Calculated mean concentration distribution along y^* for different values of the anisotropic dispersion coefficient $a = D_x/D_y$ at $x^* = 0{\cdot}5$ and $t^* = 0{\cdot}0618$ (random walk approach with $M = 1000$)

where X_i^* is the co-ordinate of the starting node i, X_j^* are the co-ordinates of neighbouring nodes j, where $j = 1, j_{max}$,

$$\alpha_1 = \frac{1/Pe_x - h^* u_x^*}{2(1/Pe_x + 1/Pe_y) - h^*(u_x^* + u_y^*)}, \tag{16b}$$

$$\alpha_2 = \frac{1/Pe_x}{2(1/Pe_x + 1/Pe_y) - h^*(u_x^* + u_y^*)}, \tag{16c}$$

$$\alpha_3 = \frac{1/Pe_y - h^* u_y^*}{2(1/Pe_x + 1/Pe_y) - h^*(u_x^* + u_y^*)}, \tag{16d}$$

$$\alpha_4 = \frac{1/Pe_y}{2(1/Pe_x + 1/Pe_y) - h^*(u_x^* + u_y^*)}, \tag{16e}$$

$Pe_x = U\,L/D_x$, $Pe_y = U\,L/D_y$, L is the length of the domain, h^* is the non-dimensional step size, u_x^* and u_y^* are the velocities in the x- and y-direction respectively and D_x and D_y are the dispersion coefficients in the x- and y-direction, respectively.

As explained above for the one-dimensional random walk method, h^* has an upper bound. The bound in the two-dimensional case is given as

$$h^* \leqslant \min\left(\frac{1}{Pe_x\,u_x^*}, \frac{1}{Pe_y\,u_y^*}\right). \tag{17}$$

The computational test for the two-dimensional case presented in this paper is performed with $h^* = 0{\cdot}08$.

Comparison with deterministic numerical method

The one-dimensional form of the differential equation (1) is solved numerically with a deterministic approach by using the PDETWO subroutine from NUMALIB.[21] This subroutine transforms the partial differential equation into an ordinary differential equation in time and then solves the ordinary differential equation for successive time steps.

Table IV shows comparatively the mean concentration computed by using the deterministic numerical, Gaussian and random walk approaches for test case I versus a set of experimental data.

Table IV. Comparison of the probabilistic and deterministic numerical solution of concentration versus experimental results at $t^* = 0{\cdot}0618$ for constant boundary conditions and random particle size ($D_{mean} = 0{\cdot}06\ cm^2\ s^{-1}$, $D_{std} = 0{\cdot}001\ cm^2\ s^{-1}$)

	Experimental[8]	Deterministic numerical approach		Gaussian approach $N = 100$, $h = 0{\cdot}1$ cm		Random walk approach $k = 0{\cdot}11$ s, $m_{max} = 45$	
x^*	C^*_{mean} (−)	C^*_{mean} (−)	ΔC^*_{mean} (%)	C^*_{mean} (−)	ΔC^*_{mean} (%)	C^*_{mean} (−)	ΔC^*_{mean} (%)
0·10	0·1524	0·1618	−6·7	0·1588	4·1	0·1440	5·5
0·20	0·6378	0·6308	−1·0	0·6274	−1·5	0·6220	2·4
0·30	0·9388	0·9296	1·0	0·9346	0·4	0·9420	−0·3
0·40	0·9960	0·9936	0·2	0·9950	0·1	1·0000	−0·4
0·50–1·0	1·0000	1·0000	0·0	1·0000	0·0	1·0000	0·0

The relative error with respect to the experimental results, ΔC^*_{mean} (%), is calculated by

$$\Delta C^*_{\text{mean}} = 100 \frac{C^*_{\text{mean}} - C^*_{\text{experimental}}}{C^*_{\text{experimental}}}. \tag{18}$$

5. CONCLUDING REMARKS

The probabilistic approach provides improved predictions for the mean parameters compared to the deterministic approach, particularly when the governing equations are strongly non-linear and the field parameters are anisotropic. At the same time, one obtains supplementary information on the probability distribution functions of the flow parameters and the effect of the spatial structure which is useful in risk analysis, occurrence of threshold processes, etc. in porous media flow. The present study with the solid phase at rest is the first step in the investigation of flows with both phases in motion, in which the randomness plays an even more significant role.

The fluctuation Peclet number Pe_{std} was defined in this paper (equations (3) and (4)) to characterize the fluctuating behaviour of the transport process. It was found that the standard deviation of the concentration solution, C^*_{std}, correlates quasilinearly with Pe_{std} in the computational test cases (Figures 12 and 13). Larger spatial correlations of the input random parameters increase the fluctuation of the solution at the same Pe_{std}.

When the transport equation is linear and isotropic, the normal and log-normal distribution functions of the diffusion coefficient in the flow field (or of concentration at the boundary) determine the normal and log-normal distributions of the field concentration, respectively. According to the chi-square test results, the corresponding concentration distributions have on average an 80% confidence level.

The non-linearity of the transport equation and the anisotropy of the field parameters determine specific effects on the first three moments of the calculated concentration distribution. The first moment is different from the equivalent deterministic solution as a function of non-linearity. The second moment (standard deviation) and third moment (skewness) are generally larger (Table II) than those of the random input parameters. The fluctuation increases with the spatial correlation (Table III).

The standard deviation of concentration at a point is directly proportional to the standard deviation of the random input parameter(s) and local gradient of the mean concentration.

ACKNOWLEDGEMENTS

This study was supported by NSF grant CBT-8511958 at the University of Kentucky.

APPENDIX: NOTATION

a	anisotropy coefficient
C	concentration
ΔC	relative error of concentration with respect to experimental results
C_b	concentration at boundary $x = 0$
C_M	maximum concentration
D_i	dispersion coefficients in the $i = x$-, y- and z-direction, respectively
d	diameter of the spheres constituting the porous material
f_d, f_{u^*}, f_{C^*}	probability density functions for D_i, u^* and C^*, respectively
F	Borel sets

h	step length in space
l_x, l_y	length of the domain in the x- and y-axis, respectively
m, M	current and total number of random walks
n_i	projection of the unit normal vector to the boundary of the ith co-ordinate
N	number of iterations in Gaussian field approach
Pe	Peclet number
$s_{\max}$	maximum number of time steps for termination of a random walk
S_N	secondary estimator
t	time
u_i	velocity in the $i = x$-, y- and z-direction, respectively
x,y,z	Cartesian co-ordinates
X_i	co-ordinate of the starting point i in random walk approach
X_j	co-ordinates of neighbouring points j in random walk approach, where $j = 1, j_{\max}$
Z	primary estimator
α_j	probability of taking a step in the jth direction, $j = 1, j_{\max}$
α	autoregressive parameter
ξ_i	random parameter at the ith iteration
Ω	population

Subscripts

i	co-ordinate ($= x$, y or z)
mean	mean quantity
std	standard deviation

Superscripts

*	non-dimensional quantity

REFERENCES

1. P. G. Saffman, 'A theory of dispersion in porous medium', *J. Fluid Mech.*, **6**, 321–349 (1959).
2. S. Whitaker, 'Diffusion and dispersion in porous media', *AIChE J.*, **13**, 420–427 (1966).
3. H. Brenner, 'The diffusion model of longitudinal mixing in beds of finite length, numerical values', *Chem. Eng. Sci.*, **17**, 229–243 (1962).
4. K. B. Bischoff and O. Lavenspiel, 'Fluid dispersion—generalization and mathematical models, 1 & 2'. *Chem. Eng. Sci.*, **17**, 245–264 (1962).
5. J. E. Warren and H. S. Price, 'Flow in heterogeneous porous media', *Soc. Petrol. Eng. J.*, **1**, 153–169 (1961).
6. L. Smith and R. A. Freeze, 'Stochastic analysis of steady state groundwater flow in bounded domain: one dimensional simulation', *Water Resources Res.*, **15**, 521–528 (1979).
7. D. H. Tang and G. F. Pinder, 'Simulation of groundwater flow and mass transport under uncertainty', *Adv. Water Res.*, **1**, 25–30 (1977).
8. A. A. Bakr, L. W. Gelhar, A. L. Gutjahr and J. R. MacMillan, 'Stochastic analysis of spatial variability in subsurface flows. I', *Water Resources Res.*, **14**, 263–271 (1978).
9. D. R. F. Harleman and R. R. Rummer, Jr., 'Dispersion permeability correlation in porous media', *ASCE Proc., J. Hydraul. Div.*, **89**, 67–85 (1963).
10. D. R. F. Harleman and R. R. Rummer, 'Longitudinal and lateral dispersion in an isotropic media', *J. Fluid Mech.*, **16**, 385–394 (1963).
11. R. R. Rummer, Jr., 'Longitudinal dispersion in steady and unsteady flow', *ASCE Proc., J. Hydraul. Div.*, **88**, 147–172 (1962).
12. O. Lavenspiel and W. K. Smith, 'Notes on diffusion type model for longitudinal mixing of fluids in flow', *Chem. Eng. Sci.*, **6**, 227–233 (1957).
13. Y. Tatsumi and Y. Suzuki, 'A case study of reliability design of a revetment by stochastic finite element method', *Proc. ICAPS 5*, 1987, pp. 970–976.

14. E. E. Alonso and G. Melloni, 'Accuracy of stochastic finite element analysis of seepage problems', *Proc. ICAPS 5*, 1987, pp. 622–639.
15. M. C. Roco and J. Khadilkar, *Probabilistic Finite Volume Method*, Research Report, University of Kentucky, 1988.
16. E. Venmarke, *Random Fields*, MIT Press, Cambridge, MA, 1983.
17. J. F. Richardson and W. N. Zaki, 'Sedimentation and fluidization', *Trans. Inst. Chem. Eng.*, **32**, 35 (1954).
18. E. Sadeh and M. A. Franklin, 'Monte Carlo solution of partial differential equations by special purpose digital computer', *IEEE Trans. Comput.*, **23**, 389–397 (1974).
19. F. L. Stasa, *Applied Finite Element Analysis for Engineers*, CBS Publications, New York, 1985.
20. O. E. Percus and J. K. Percus, 'One dimensional random walk with phase transition', *SIAM J. appl. Math.*, **40**, 485–497 (1981).
21. PDETWO, Subroutine from the Library NUMALIB, University of Kentucky Computing Center, 1986.